Electrical and spectroscopic analysis in nanostructured SnO_2: "Long-term" resistance drift is due to in-diffusion

Cesare Malagù,[1,2,a)] Alessio Giberti,[1] Sara Morandi,[3] and Celso M. Aldao[4]
[1]*Department of Physics, University of Ferrara, Via Saragat 1/c, Ferrara 44100, Italy*
[2]*IDASC - Istituto di Acustica e Sensoristica "O. M. Corbino," Italy*
[3]*Department of Inorganic, Physical and Materials Chemistry and NIS Centre of Excellence, University of Turin, Via P. Giuria 7, Torino 10125, Italy*
[4]*Institute of Materials Science and Technology (INTEMA), University of Mar del Plata and National Research Council (CONICET), Juan B. Justo 4302, Mar del Plata B7608FDQ, Argentina*

(Received 21 March 2011; accepted 7 October 2011; published online 7 November 2011)

A model for conductance in *n*-type non-degenerate semiconductors is proposed and applied to polycrystalline SnO_2 used as a gas sensor. Particular attention is devoted to the fundamental mechanism of Schottky barrier formation due to surface states in nanostructured grains. Electrical and absorption infra-red spectroscopic analysis constitutes strong evidence for oxygen diffusion into the tin oxide grains. The model is then extended to include oxygen in- and out-diffusion. Thus, it is possible to explain the "long-term" resistance drift in oxygen for fully depleted grained samples in terms of tunneling through the double barrier. © *2011 American Institute of Physics*.
[doi:10.1063/1.3658870]

I. INTRODUCTION

Studies of electron transport through metal-semiconductor interfaces date from the discovery of rectifying contacts.[1–3] While important advances have been made in understanding Schottky barrier formation,[4] the physical details behind these phenomena have remained elusive, especially when states at the interface play a dominant role. Conduction models in polycrystalline materials,[5] nanostructured materials,[6] photoemission from negative-electron-affinity materials,[7] and gas sensing via chemoresistive materials[8] depend on such atomistic details. Double Schottky barriers include even more complexities, and there are several key questions that remain.

This paper focuses on the mechanism of double Schottky barrier formation at the interface semiconductor-gas-semiconductor in polycrystalline SnO_2 and provides some important new insights. As nanometric dimensions are reached, the average grain radius can be as large as the depletion width. Then, grains can be completely depleted of carriers affecting the conduction mechanisms, which have been missed in the past. Through a theoretical and experimental approach, we will present the relevant mechanisms responsible for the observed results. We will first discuss the adsorption of oxygen at surface (O^-) and its role in the observed increase in resistance.[9,10] Then, FTIR results, not explicable simply by surface desorption/adsorption of oxygen species, will be shown to be an evidence of oxygen in- and out- diffusion in the bulk of SnO_2 grains.

II. EXPERIMENTAL

A pure SnO_2 sample was prepared through a modified sol-gel process described as follows: to an n-butanol solution 0.7 M of tin(II)2-ethylex-anoate (Strem Chemicals), a given amount of de-ionized water was added drop-wise, and the mixture was stirred at room temperature (RT) for 3 h. The molar ratio of water to Sn was 4 and the pH of the solution was adjusted to be 1 with HNO_3. The resulting gel was dried overnight at 95 °C, giving a yellow powder. The powder was subsequently calcined at 550 °C for 2 h.

Absorption IR spectra were run at different temperatures on a Perkin-Elmer System 2000 FTIR spectrophotometer equipped with a Hg-Cd-Te cryodetector, working in the range of wavenumbers 7800–580 cm^{-1} at a resolution of 2 cm^{-1}. For FTIR analysis, the powder was compressed in a self-supporting disk and placed in a commercial heated stainless steel IR cell (Aabspec), allowing thermal treatments *in situ* under vacuum or controlled atmosphere and the simultaneous registration of spectra at temperatures up to 600 °C. The sample was first treated at 400 °C in vacuum and in dry oxygen to clean the surface from adsorbed species. After this activation stage, the sample was cooled down to RT in oxygen and FTIR spectra were run during the subsequent outgassing in the temperature range RT-300 °C with steps of 50 °C. After these treatments in vacuum, the sample was cooled down again to RT and oxygen (20 mbar) was admitted. FTIR spectra were run in oxygen at increasing temperature in the range RT-300 °C with steps of 50 °C. It is important to point out that FTIR spectra are reported in the figures as difference spectra, where the subtrahend spectrum is always that of the sample outgassed and oxidized at 400 °C. This elaboration is useful to put in evidence only the changes induced by the treatments.

The thick film employed in the electrical measurements was prepared starting from a paste obtained by adding to the SnO_2 powder an organic vehicle together with a small percentage of glass frit for improving the adhesion of the layers to the substrates. The film was screen-printed onto alumina substrate (2.5×2.5 mm^2), provided with a heater element on

a)Author to whom correspondence should be addressed. Electronic mail: malagu@fe.infn.it.

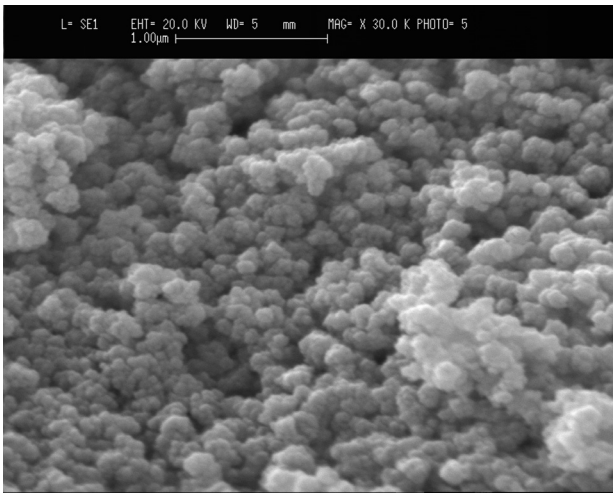

FIG. 1. SEM micrographs of SnO_2 film with average radius (50 nm).

the backside and gold front interdigitated contacts, and was fired in air at 650 °C for 1 h. The thickness of the resulting film was about 30 μm. Figure 1 shows a SEM image of the microstructure of the sample; from this, we determined an average grain radius of about 50 nm. Stoichiometry of the prepared SnO_2 was confirmed by x ray diffraction (as reported in Ref. 11) performed on the material using a vertical diffractometer (Philips PW 1820/00) equipped with an x ray source operating at 1000 W (using a Cu K radiation with $\lambda = 1.54$ A°). The sensor was placed in a sealed test chamber equipped for flow-through technique,[12] which, in turn, was placed in a thermostatic chamber to keep room temperature fixed at 27 °C. The electrical measurements were performed as follows: pure nitrogen was injected at a flow rate of 100 sccm in the sealed chamber until the stabilization of the conductance was reached, then the flow was switched to 100 sccm of dry synthetic air with a flow meter. The volume of the test chamber is 500 cm^3, so that the time scale of the presented measurements is sufficiently larger than the ratio between volume and flow rate, thereby the response time is not affected by it. The sensor bias was kept fixed at 2.5 V with an operational amplifier, and the output signal was measured through a KEITHLEY 2000 Multimeter. The resistance variation of the film was measured at four working temperatures.

III. THEORETICAL BACKGROUND AND MODEL

Reference 13 showed that the interpretation of conductivity in nanocrystalline semiconductors neglects an important contribution, namely the tunneling contribution. The tunneling contribution, here called I_1, and the thermionic one, here called I_2, turned out to be

$$I_1 = \frac{qV_S}{K_BT}\int_0^1 Exp\left\{-\frac{qV_S}{K_BT}\left[\alpha + \frac{2K_BTy(\alpha)}{E_{00}}\right]\right\}d\alpha,$$
$$I_2 = Exp\left(-\frac{qV_S}{K_BT}\right), \tag{1}$$

where

$$y(\alpha) = (1-\alpha)^{0.5} - \alpha \ln\left[\frac{1+(1-\alpha)^{0.5}}{\alpha^{0.5}}\right],$$
$$\alpha = \frac{E}{qV_S}, \tag{2}$$
$$E_{00} = \frac{qh}{4\pi}\left(\frac{N_d}{m_n\varepsilon}\right)^{0.5},$$

E being the energy of an electron in the conduction band, q the electronic charge, k_B the Boltzmann constant, h the Plank constant, T the absolute temperature, V_s the surface potential barrier, N_d the doping level, m_n the effective electron mass, and ε the permittivity.

It is generally acknowledged[9] that the main adsorbed charged oxygen species is O^-, so the relevant reactions are regularly reduced to[14]

$$O_2(g) + 2S + 2e^- \Leftrightarrow 2O^-(a), \tag{3}$$

where S corresponds to adsorption sites at the surface, (g) refers to the gas phase, and (a) to an adsorbed species. Equation (3) states that more oxygen in the ambient implies a larger amount of chemisorbed oxygen and, thus, higher inter-granular barriers.

According to Bardeen's model, discussed in Ref. 15, a neutral level for the surface states, ϕ_o, is defined such as the surface states above it are acceptor-like (neutral when empty) and those below are donor-like (neutral when full). The approximation that gap states above Fermi level, E_F, are empty and states below are full holds. In the case of SnO_2, when surface states are present at the bandgap, electrons of the conduction band become trapped in the surface acceptors, as described in Eq. (3), and the conduction band bends, increasing its distance from E_F. Thus, a depletion region, whose width is called Λ, develops where the electron density is very low (Fig. 2). At equilibrium, the position of ϕ_o with respect to the conduction band, E_c, at surface is constant for a given atmosphere and working temperature, independently of the built-in potential. In this condition, the surface states

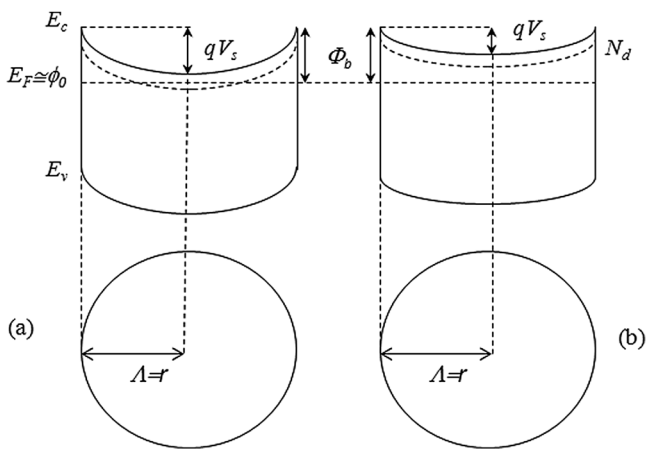

FIG. 2. Band bending in fully depleted grains ($\Lambda = r$). (a) qV_s is almost equal to Φ_b, and the second ionization level of oxygen vacancies is below E_F near the center of the grain. (b) When oxygen in-diffusion lifts E_c with respect to E_F, qV_s becomes smaller than Φ_b and the vacancies are doubly ionized in the whole grain.

below E_F and above ϕ_o are full and acceptors; thus, they constitute the negative net surface charge that compensates the positive space charge.

The surface density of negatively charged states, $N_s = [O^-]$, is then given by the product of the energy density of surface states, D_{ss}, with the interval of energies where the charged surface states are present,

$$N_s = D_{ss} \times (E_F - \phi_0). \tag{4}$$

If D_{ss} is very large, E_F tends to ϕ_o and the Schottky barrier, which is, by definition, $E_c(surf)$-E_F, is univocally determined by ϕ_o. This is the so-called pinning of Fermi level, which means that the Schottky barrier, Φ_b, is determined only by the position of the neutral level in the gap and becomes independent of the built-in potential V_s;[15] compare Figs. 2(a) and 2(b): Φ_b stays the same, even if the built-in potential, V_s, is much smaller in case (b).

Indeed, oxygen vacancies are the dominant defects, and they behave as donor impurities, the density of which is N_d. The oxygen exchange equilibrium is regularly written as[16]

$$O_0 \Leftrightarrow V^{++} + 2e^- + \frac{1}{2}O_2, \tag{5}$$

where V^{++} is a double ionized vacancy, e^- is an electron, O_2 an oxygen molecule, and O_o oxygen at lattice site. The corresponding mass action law is

$$K = [V^{++}][e^-]^2 p(O_2)^{\frac{1}{2}}. \tag{6}$$

Square brackets denote concentrations, K is the mass action constant, and $p(O_2)$ is the oxygen partial pressure. Despite its general use, Eq. (5) does not tell us of the mechanism by which bulk oxygen reaches the surface and then the gas phase (and the inverse process). This mechanism is supposed to be the diffusion of oxygen interstitials.[17] Thus, the square root of $p(O_2)$ represents the concentration of in- and out-diffusing interstitial oxygen atoms, $[O_i]$.

It is apparent from Eq. (6) that oxygen interstitials alter the oxygen vacancies concentration, $[V] = N_d$ and then the depletion region width, Λ. However, this mechanism cannot modify the barrier height, since equilibrium at surface has already been established by Eq. (3), which is supposed to have quicker kinetics and, if the energy density of surface states is sufficiently high, E_F is pinned at ϕ_0. Only the depletion width, Λ, can be modified: as oxygen vacancies are filled by interstitial in-diffusing oxygen, Λ increases as long as it reaches the value of the grain radius, r, and the grain becomes fully depleted (see Fig. 2(a)). From this moment on, the conduction band bottom, E_c, at the center of the grain starts to move far from the E_F (see Fig. 2(b)). The mechanism can go on until the flatband condition is reached. The diffusion of oxygen interstitials in and out of the grains must be possible because of the observed reversibility in gas sensor experiments.[18]

Once this point has been clarified, it can be accepted that oxygen in-diffusion just modifies the doping level, and the only effect is to increase the depletion width until it reaches $\Lambda = r$; after that, the in-diffusion pushes the bottom of the conduction band at the center of the grain away from E_F (see Fig. 2(b)). In fact, see Eq. (1); the term I_2 increases exponentially as qV_s is decreased, but at the same time, the density of electrons in the grain decreases exponentially as E_c increases its distance from E_F at the center of the grain. The two effects compensate exactly if $E_c(surf)$-E_F is kept constant; thereby, the thermionic contribution to conductivity cannot change if the Schottky barrier height, Φ_b, is constant. The only affected term is the tunneling contribution to conductivity, I_1 in Eq. (1), because the electrons at a fixed energy distance from the E_F see a relatively larger barrier to tunnel through and the tunneling contribution is decreased.

IV. RESULTS AND DISCUSSION

The electrical measurements are reported in Fig. 3. After stabilization is reached in nitrogen, 20% oxygen is injected and the first increase in resistance is observed at all working temperatures. At the lower temperatures (Figs. 3(a) and 3(b)), the net difference between the two slopes of resistance increase is not very evident, whereas at 400 °C (Fig. 3(c)), it becomes apparent. At 500 °C (Fig. 3(d)), the presence of two different time constants is even clearer. Two phenomena are acting together: a more rapid surface effect, whose equilibrium is described by Eq. (3), and a slower bulk in-diffusion, which lasts many hours and is determined by Eq. (5). The surface phenomenon becomes clearly quicker than the other one only at the two highest temperatures.

The continuous increase in the resistance, after surface equilibrium, is explained in the theoretical section: pinning of E_F keeps Φ_B constant, and the thermionic contribution to resistance cannot change. As oxygen atoms in-diffuse in the bulk of the grains, the transition between, in Fig. 2(a) to Fig. 2(b), leads to tunneling contribution decrease.

In order to verify oxygen in- and out-diffusion in SnO_2, FTIR analysis has been performed, as described above. The results are reported in Fig. 4. A broad absorption band centered at about 1600 cm^{-1} ($\sim$0.2 eV) increases in intensity on increasing the out-gassing temperature (Fig. 4(a)). The subsequent treatment in oxygen (Fig. 4(b)) at increasing temperature gradually erodes this band, putting in evidence that the observed behavior is related to the loss and recovering of oxygen. The energy of the absorption is consistent with the second ionization of oxygen vacancies in SnO_2 (0.15 eV).[19]

In the following, it will be shown that FTIR results can be explained on the basis of in- and out-diffusion mechanism (Eq. (5)) and not only by considering oxygen adsorption at the surface (Eq. (3)).

In the central part of a grain in the condition of Fig. 2(a), E_F is close to the bottom of the conduction band (E_c); say that E_c–E_F is about 0.1 eV. The dotted line which follows the profile of band bending represents the second ionization level for oxygen vacancies. Therefore, vacancies near the center of the grain are singly ionized because their level is below E_F, whereas vacancies near the surface are doubly ionized because their level is above E_F.

When the bands flatten because of oxygen in-diffusion (Fig. 2(b)), E_F is below the second ionization level along the whole grain. Thus, vacancies are almost all doubly ionized.

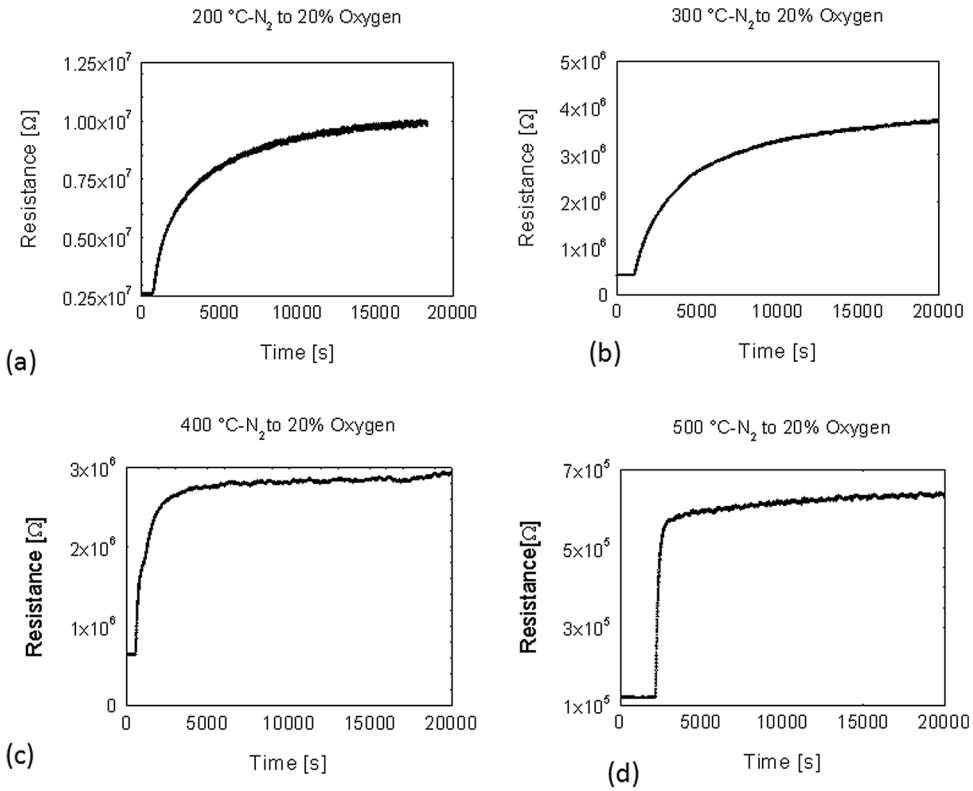

FIG. 3. Electrical responses to 20% of O_2 in nitrogen. (a) 200 °C, (b) 300 °C, (c) 400 °C, (d) 500 °C.

The experiments of Fig. 4(a) **start** with a sample having grains (50 nm) completely depleted, with the Fermi level below the vacancy second ionization level along the whole grain. Then, there are very few singly ionized vacancies, as shown in Fig. 2(b), and IR absorption is negligible. Vacuum is made and temperature is raised: a rapid oxygen desorption from the grain surface occurs, which is responsible for reducing Φ_B, then oxygen out-diffusion takes place, vacancy density increases, and E_c approaches E_F at the center of the grain. Thus, singly ionized vacancies appear and their density increases as out-diffusion continues. The final situation, represented in Fig. 2(a), is that observed at 300 °C with the highest intensity of the IR absorption band (Fig. 4(a), curve 6).

At this point, the temperature is reduced to RT and the system corresponds to the initial situation for Fig. 4(b) (curve 1), again represented in Fig. 2(a). Now, as temperature is raised in an ambient with oxygen, the inverse process occurs, e.g., the presence of oxygen increases the amount of adsorbed oxygen at the grain surface. Then, Φ_B increases; after that, in-diffusion is responsible for the recovery of the initial situation described in Fig. 2(b). Therefore, most of the original oxygen is recovered, the conduction band minimum is raised, vacancies are doubly ionized, and the IR absorption is very small again.

The behavior in oxygen of the IR absorption related to the second ionization of oxygen vacancies could not be

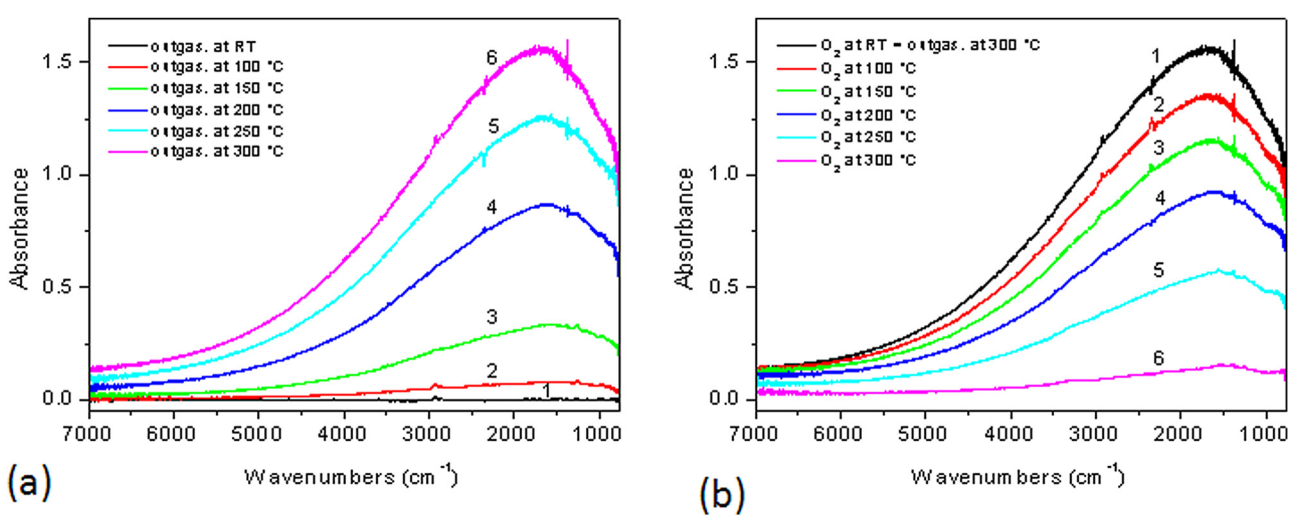

FIG. 4. (Color online) Difference in FTIR spectra: (a) outgassing in vacuum at increasing T; (b) subsequent treatment in O_2 (20 mbar) at increasing T. Outgassing and oxidation treatments were performed at RT (curves 1), 100 °C (curves 2), 150 °C (curves 3), 200 °C (curves 4), 250 °C (curves 5), and 300 °C (curves 6).

explained by surface adsorption. Indeed, on the basis of literature information, O_2^- adsorbed species is converted into O^- adsorbed species at about 150 °C.[20] Then, the transformation into O^{2-} species occurs at about 450–500 °C. For these reasons, in the temperature range 150–300 °C, it is possible to consider that only O^- species are present at the grain surface and, reasonably, its amount decreases or at least remains constant with the temperature raise. As a consequence, if surface adsorption was the only mechanism present, the IR absorption band would decrease in oxygen until 150 °C, then, at a higher temperature, it would increase again or at least remain constant. This is not the case, confirming the in-diffusion of oxygen and out-diffusion for treatment in vacuum or inert atmosphere.

V. CONCLUSIONS

In this work, we presented a model for thermionic and tunneling barrier crossing in *n*-type polycrystalline SnO_2 exposed to vacuum- and oxygen-rich environments. We have proposed two mechanisms, with two different kinetics, responsible for resistance variation, depending on dynamical equilibrium between gas and semiconductor:

a) The first one (surface state effect with quicker time constant) is responsible for the barrier height, i.e., distance of the conduction band bottom at surface from the Fermi level.
b) The second one is between bulk and gas (in-diffusion effect with longer time constant) and is mainly responsible for the barrier shape through the increase of Λ.

The resistance variations are interpreted in terms of these mechanisms. The second mechanism shows that the density of oxygen vacancies only depends on oxygen partial pressure and time.

Thermionic contribution to conductivity is not affected by the shape of the barrier, but tunneling is; this explains the long time drift in the resistance observed at all working temperatures. The spectroscopic infrared analyses confirmed the in- and out-diffusion of oxygen atoms that affects the doping level and, thus, the film resistivity through the tunneling contribution to the total current density.

[1]F. Flores, Surf. Rev. Lett. **2**, 513 (1995).
[2]L. J. Brillson, in *Handbook of Semiconductors*, edited by T. S. Moss (Elsevier, Amsterdam, 1992).
[3]E. H. Rhoderick and R. H. Williams, in *Metal-Semiconductor Contacts* (Oxford Science Publications, Oxford, 1988).
[4]K. Stilies and A. Khan, Phys. Rev. Lett. **60**, 440 (1988).
[5]J. Y. W. Seto, J. Appl. Phys. **46**, 5247 (1975).
[6]J. L. Solis, A. Hoel, V. Lantto, and C. G. Granqvist, J. Appl. Phys. **89**, 2727 (2001).
[7]L. Diederich, P. Aebi, O. M. Kuttel, and L. Schlapbach, Surf. Sci. **424**, L314 (1999).
[8]C. Malagù, V. Guidi, M. Stefancich, M. C. Carotta, and G. Martinelli, J. Appl. Phys. **91**, 808 (2002).
[9]N. Yamazoe and K. Shimanoe, Thin Solid Films **517**, 6148 (2009).
[10]G. Blaustein, M. S. Castro, and C. M. Aldao, Sens. Actuators B **55**, 33 (1999).
[11]M. C. Carotta, S. Gherardi, V. Guidi, C. Malagù, G. Martinelli, B. Vendemiati, M. Sacerdoti, G. Ghiotti, S. Morandi, A. Bismuto, P. Maddalena, and A. Setaro, Sens. Actuators B **130**, 38 (2008).
[12]V. Guidi, M. A. Butturi, M. C. Carotta, B. Cavicchi, M. Ferroni, C. Malagù, G. Martinelli, D. Vincenzi, M. Sacerdoti, and M. Zen, Sens. Actuators B **84**, 72 (2002).
[13]C. Malagù, G. Martinelli, M. A. Ponce, and C. M. Aldao, Appl. Phys. Lett. **92**, 162104 (2008).
[14]T. Sahm, A. Gurlo, N. Barsan, and U. Weimar, Sens. Actuators B **118**, 78 (2006).
[15]T. G. G. Maffeıs, G. T. Owen, C. Malagù, G. Martinelli, M. K. Kennedy, F. E. Kruis, and S. P. Wilks, Surf. Sci. **550**, 21 (2004).
[16]B. Kamp, R. Merkle, and J. Maier, Sens. Actuators B **77**, 534 (2001).
[17]C. M. Aldao, D. A. Mirabella, M. A. Ponce, A. Giberti, and C. Malagù, J. Appl. Phys. **109**, 063723 (2011).
[18]M. C. Carotta, A. Giberti, V. Guidi, C. Malagù, B. Vendemiati, G. Martinelli, Mater. Res. Soc. Symp. Proc. **828**, 173 (2005).
[19]J. Mayer and W Göpel, J. Solid State Chem. **72**, 293 (1988).
[20]G. Sberveglieri, in *Gas Sensors, Principles, Operation and Development* (Springer, New York, 1992), pp. 145–146.